Journal of Thermal Analysis and Calorimetry, Vol. 68 (2002) 223–230

CALORIMETRIC STUDY OF FROST ATTACK DURING CEMENT HARDENING*

A. Usherov-Marshak, O. Zlatkovski and V. Sopov

Chair of Physical-Chemical Mechanics and Technology of Building Materials and Products, Kharkov State Technical University of Building and Architecture, Sumskaya ul. 40, 61002 Kharkiv, Ukraine

Abstract

This report deals with practical and experimental studies of the effects of frost attack on hardening cement stone and concrete. The basic component of concrete, cement stone, is a typical capillary-porous material formed from solid, liquid and gaseous phases. The level of knowledge on the effects of frost attack on cement stone and concrete hardening is insufficient, due to the complexity of the mechanisms of the accompanying effects. The values of internal pressures are determined among others by ice formation parameters, by the characteristics of the porous structure and the solid phase of the cement stone, and also by technological factors. The quantitative estimation of certain parameters is important for an approach to the understanding of the mechanism of frost attack and the choice of methods of its regulation for technological purposes. These are the temperature of pore liquid crystallization T_f, the degree of freezing F_d and the mass of ice I_m formed during freezing. Examples of changes in ice formation parameters on variation of some of the technological factors are given.

Keywords: differential scanning calorimetry, frost attack, ice formation, pore solution

Introduction

Cement stone is a capillary-porous material formed from solid, liquid and gaseous phases. Concrete operations in wintertime are subject to the action of frost, and ice formation in the pores is a source of interior stresses. Various hypotheses have been proposed to explain the mechanisms of frost attack. The cooling of cement stone is accompanied by the development of thermal stresses, and hydraulic, crystallizational [1] and osmotic [2, 3] pressures. One reason for the osmotic pressure is the increase in density of dissolved ions in the not-frozen water during the formation of ice chips in the pores. As the ice is formed and the volume expands, crystallizational pressure builds up in the closed pores. The hydraulic pressure develops when a liquid phase is pressed into a pore system unfilled by water. The characteristics of porosity and the solid phase and also the parameters of ice formation determine the magnitude of the pressure and the accompanying risks to the stability of the concrete structure.

* Paper was presented at CCTA 8, Zakopane (Poland) September, 2000

1418–2874/2002/ $ 5.00

Akadémiai Kiadó, Budapest
Kluwer Academic Publishers, Dordrecht

Theoretical basis

In response to the effects of surface forces the properties of a pore solution vary in a different way from those of a bulk solution [4–7]. In particular, the temperature and heat of crystallization are reduced. The thermodynamic correlation between the temperature of crystallization and the radius of the pores indicates that the temperature of crystallization of a pore solution T_f is an important parameter of ice formation. The relation between the temperature of crystallization of a pore solution and the temperature of the environment determines the occurrence and the degree of completeness of the ice formation process. It indirectly establishes a temperature limit of cooling of cement stone.

When the ice formation process occurs, the absolute and relative values of the mass of ice generated, I_m, and the degree of freezing, F_d, predominate. I_m corresponds to the total amount of water frozen in the cement stone. It determines the magnitudes of the hydraulic and crystallizational pressures. The amount of frozen water, H_2O_{fr}, characterizes the mass of connected water, H_2O_{con}. F_d reflects the frozen pore fluid in relation to the common mass of water in the pores, i.e. the mass ratio of the free water to the sum of the free and adsorbed water. The parameters I_m, F_d and T_f are interconnected and depend on the porosity. T_f is determined by the size of the pores. The magnitude of F_d characterizes the distribution of the pores by size. I_m reflects the volume of the pores, completed by water. The correlation between them is given by the 3-dimensional ITF model (Fig. 1).

The model is constructed as follows. A circle is placed on the plane formed by the coordinate axes ‘mass of ice’ and ‘degree of freezing’. The position of its centre is determined by the values I_m and F_d. The radius and brightness of the circle are deter-

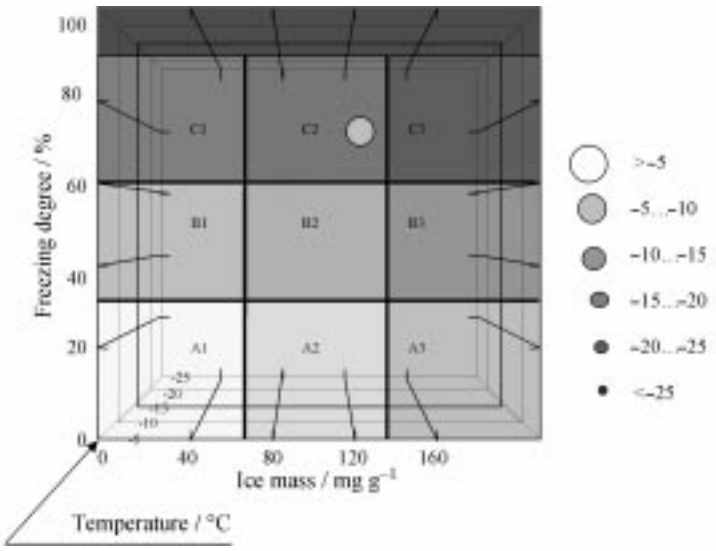

Fig. 1 ITF model of ice formation

mined by the magnitude T_f, as in Fig. 1. To a first approximation, the radius of the circle is inversely proportional to the temperature of crystallization. A similar association links the absolute value of temperature of crystallization and the pore radius [4]. Thus, the larger the circle, the more the dominant pore radius. The circle is an important element of the model and is regarded as the 'reflex' of a sample in the space of the ITF model.

As an example, Fig. 1 depicts the reflex for a sample of cement stone with the following parameters: T_f= –4°C, I_m=120 mg g^{-1}, F_d=75%.

In the map of the risk of ice formation, the space is broken down into 10 zones, depending on the values of the ice mass and the degree of freezing (Fig. 1). The brighter a site, the less the risk of development of negative features on cooling.

Experimental procedure

The method of differential scanning calorimetry (DSC) was applied for the experimental determination of the parameters of ice formation. At the freezing of a cement stone, certain elementary thermodynamic processes influence the internal energy. These are the cooling of the structural phases of cement stone, the solid matrix, the non-frozen water and the ice formed, and also the crystallization of the pore fluid. The resulting change in the internal energy is described by the differential equation of heat balance:

$$dH = dT[m_c c_c(T) + (m_w^0 - m_w(T))c_w(T) + m_i(T)c_i(T)] + \partial m_i L(T) \quad (1)$$

where m_c – mass of cement stone, m_w^0 – initial mass of water, $m_w(T)$ – mass of ice formed up to temperature T, ∂m_i – increment of mass of ice, $c_c(T)$, $c_w(T)$ and $c_i(T)$ – specific calorific capacities of cement stone, water and ice, respectively, dT – increment of temperature for a pitch, and $L(T)$ – specific heat of crystallization.

DSC allows the recording of a thermal flow on a change of temperature of a sample. Thus, the phase transformations of water are displayed at defined temperatures as maxima on the background noise of the baseline. The mass of generated ice I_m is found from (1). The degree of freezing of a pore fluid is determined from the knowledge of its structure. A pore fluid is represented as quasi-free nucleus, which is overlapped by a thin layer of adsorbed water on the internal walls of the pores. Internal quasi-free water is freezable water. Adsorbed water does not freeze until –90°C. As water in gel pores freezes at temperatures near –50°C, under actual winter conditions it does not freeze. Thus, the degree of freezing is equal to the ratio of the mass of freezable water to the sum of the free water, the water in the adsorbed layer and the water in the gel pores.

Samples of cement paste with the necessary water-to-cement ratio, with a mass of about 20–40 mg, were packed in pressurized aluminum containers. After a sufficient time of hardening under pre-given conditions, they were frozen with the use of liquid nitrogen at some rate of cooling in the range 0.5–2.0°C min^{-1}. During this, the rate of heat dH/dt necessary to keep the temperatures of the sample and the control

specimen equal was measured. As a result of this experiment, we obtained the dependency $I_m - f(T)$, and the values of parameters I_m, T_f and F_d.

Results and discussion

The characteristics of ice formation were investigated during the setting of hardening binders: tricalcium silicate, $3CaO \cdot SiO_2$ (C_3S), tricalcium aluminate $3CaO \cdot Al_2O_3$ (C_3A), and cement. The effects of technological factors, such as the time of setting, the water–solid ratio (*W*/*S*), the curing conditions before setting and the role of chemical components (antifreezes) on the parameters of the process were estimated.

At the freezing of samples based on C_3S, two maxima were recorded, in the temperature intervals –7...–11 and –45...–50°C. The second maximum does not occur at once, but after 2–3 days of hardening. In the early stages, only one range of pore size was observed: 12–30 nm. During hydration, the pores become filled by gel. The distribution curve of the pores by size exhibits two maxima: for gel pores with a radius of about 2–6 nm and for meso-capillaries with a radius of 12–20 nm.

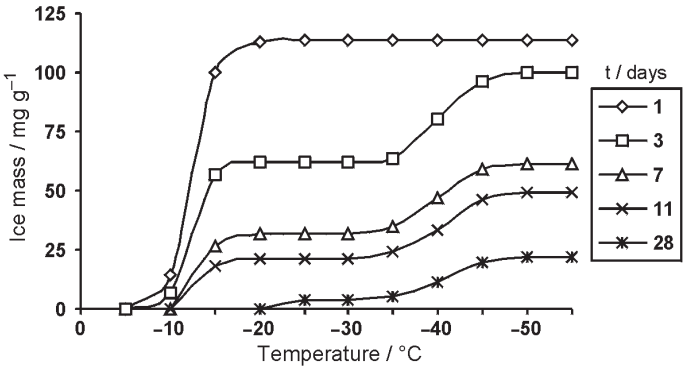

Fig. 2 Ice formation during hardening of C_3S

On lengthening of the hardening time under normal conditions, the amount of ice generated during freezing I_m is decreases: during 7 days, up to 50% of ice is formed in the gel pores (Fig. 2).

From analysis of the ITF model (Fig. 3), it follows that, during the process of hydration, the reflexes of samples based on the hardening of C_3S are shifted from a zone of high risk 'C' to a zone 'A', with smaller indices of the risk of ice formation. The values of all parameters decrease.

The distribution of the pore sizes and the character of ice formation in samples based on C_3S, with two local maxima, point to the origin of the hydraulic pressure. On the freezing of a fluid in the structural elements of $Ca(OH)_2$, ice forces are transmitted through the not-frozen water in the air pores in the pore system of a hydrosilicate gel.

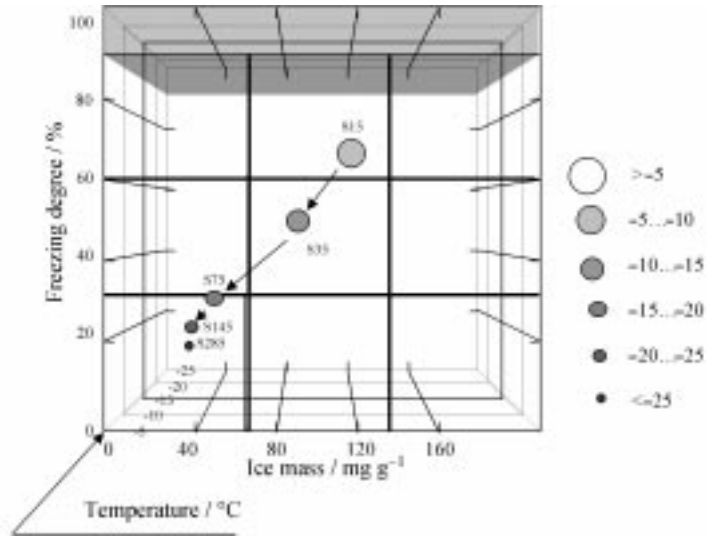

Fig. 3 ITF model for estimation of ice formation during setting of samples based on C_3S

The character of the shaping of the structure essentially differs in the hardening of C_3A. The structure of hydroaluminates of calcium with large (20–70 nm) capillaries is reflected by the presence of one maximum of ice formation, at –3...–7°C (Fig. 4). The similar character of ice formation does not lead to the development of hydraulic pressure. The pressure on water during the growth of chips of ice is transmitted immediately to a solid matrix. The probability of the development of crystallizational and osmotic pressures increases. Thus, the osmosis due to a higher density of ions requires the intake of water from the outside or the slowing-down of ice formation. However, the lower durability of the hydroaluminate of calcium can promote the formation and development of imperfections in the structure.

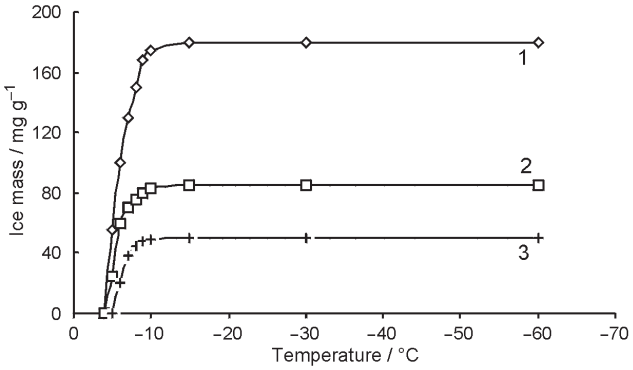

Fig. 4 Ice formation during setting of samples based on C_3A. 1, 2, 3 – duration of hardening before setting: 3, 24 h and 7 days, respectively

The temperature of crystallization of a pore fluid practically does not vary with the duration of hardening, and is –5...–6°C. The mass of ice I_m is reduced from 145 mg g^{-1} for samples after 2 h to 60 mg g^{-1} for a 7-day sample. T_f and F_d practically do not vary. The reflexes of frozen samples based on C_3A within the ITF model do not fall outside the limits of the danger zone 'C'.

In cement stone, the interacting structures (hydrosilicate, hydroaluminate and hydrosulfoaluminate) are shaped. The hydration of the cement paste results in poorly shaped colloidal particles and insignificant amounts of rather large crystalline plates of CH and sulfoaluminates. It has been reported [8] that the basic products of hydration of Portland cement are C_2SH_2, CSH(B), C_3AH_6, $C_4AH_{11–19}$ and $Ca(OH)_2$.

The distribution of the pore sizes in cement stone is characterized by two maxima. That in the interval 1.5–4 nm corresponds to the micropores of a gel, and that at 10–50 nm to capillaries inside and between crystalline inclusions. At freezing two peaks of ice formation are observed, at –5...–12 and –45...–55°C. Under identical conditions, the mass of ice in cement stone is higher than that in stone from C_3S; this confirms the view of Grudemo [9]. On lengthening of the duration of hardening of cement stone, the mass of ice generated at freezing is reduced. For samples frozen after 1, 3, 7 and 28 days, I_m is 130, 105, 60 and 25 mg g^{-1}, respectively. During 3 days, 45% of the water in the gel pores, and during 28 days, 80% of all the water is converted to ice. The values of I_m and T_f are influenced most by the content of C_3A. For example, on increase of the C_3A content in a cement, from 6.5 up to 9%, the mass of ice in the cement stone rises from 75 to 140 mg g^{-1}.

I_m is diminished most intensively during the first 3–4 h, from 333 to 210 mg g^{-1}, i.e. by 123 mg g^{-1}. Then, during 20 h a significant slowing-down of the process is observed. Up to 24 h, the mass of ice is reduced to 190 mg g^{-1}, i.e. by only 20 mg g^{-1}. The similar character of the change in the mass of ice confirms the necessity to protect concrete from operations at negative temperatures during the first 4–6 h.

The content of liquid phase and the water–solid (water–cement for cements) ratio largely determine the ability of concrete to resist frosting attack. The data in Fig. 5 reflect the influence of the water–solid ratio (*W*/*S*) on the parameters of ice formation

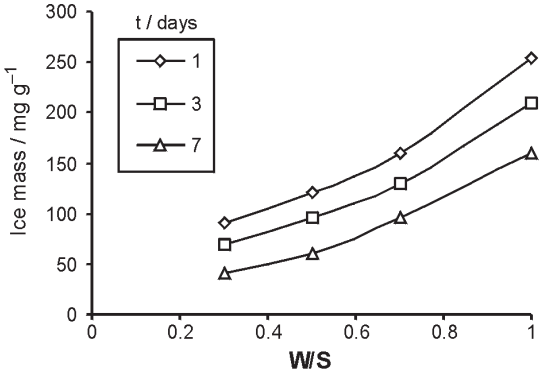

Fig. 5 Influence of *W*/*S* on amount of ice in frozen samples of hardening cement stone

during the freezing of samples of cement stone. On the increase of *W*/*S*, only the absolute indices of the ice mass I_m rise.

The ratio *W*/*S* does not influence the character and temperature interval of phase transformations of a pore fluid on the setting of cement stone. Its change leads to horizontal displacement of the reflexes in the ITF model. This indicates that variation of the water–solid ratio causes a change in the amount of pores, without a change in the character of the size distribution.

Heat-moisture handling of concrete, as a means of accelerating hardening, results in a change in the structure of the cement stone. An elevation of temperature does not have an essential effect on the structure of new formations as contrasted to hardening under normal conditions, but can lead to a more defective structure with a heightened denseness of diffusion envelopes. It can enhance the risks at freezing. When hardening is carried out at +80°C, two transformations are observed: in the intervals –6...–9 and –40...–45°C. Intensification of hydration by the elevation of temperature results in crystallization of the pore fluid occurring at temperatures 3–4°C higher than in samples undergoing normal hardening.

In the technology of winter concreting at negative temperatures, anti-frost admixtures with electrolytes are applied with high effectivity. They reduce the temperature of crystallization of the pore fluid and ensure a shaping structure, capable of resisting frosting action. The temperature of crystallization of pore fluid in the presence of 10% of K_2CO_3 is reduced from –7 to –18°C. At the same time, the mass of generated ice and the degree of freezing are diminished by only 5–10%.

Conclusions

To account for the various mechanisms of frost destruction, it is recommended that the risk of ice formation is evaluated by a complex of three parameters: the temperature of crystallization of the pore solution, the degree of freezing and the mass of ice generated at freezing.

The regularities and parameters of ice formation during the freezing of hardening binders and their changes in response to various technological factors have been investigated by means of differential scanning calorimetry.

References

1 T. C. Powers, A working hypothesis for future studies of frost resistance of concrete, J.ACI Proc., 1945, p. 245.
2 O. E. Vlasov, An equilibrium of a multicomponent and multiphase capillary system. Durability of protecting and building constructions (physical fundamentals), Moscow 1963, p. 6.
3 V. I. Babushkin, A defense of building constructions from corrosion, aging and wear, High School Publ. at Kh. Un-t, Kharkov 1989, p. 168.
4 A. Adamson, Physical chemistry of a surface, Mir, Moscow 1974.
5 E. J. Sellevold and D. H. Bager, Low temperature calorimetry as a pore structure probe, Proc. 7th ICCC, Vol. 4, Paris 1980, p. 394.

6 N. Stockhausen, H. Dorner, B. Zech and M. J. Setzer, Cem. Concr. Res., 9 (1979) 783.
7 M. Brun, A. Lallimand, J. F. Quinson and Ch. Eyard, Thermodinamica Acta, (1977) 21.
8 L. L. Shpynova, V. I. Chih and M. A. Sanitsky, Physical-chemical basis of formation of structure of cement stone, High School, Lvov 1981.
9 A. Grudemo, Microstructure of hardening cement paste, IV ICCC, 1964.